

Nonlinear analysis using load-displacement control

Young-Doo Kwon[†]

School of Mechanical Engineering, Kyungpook National University, Daegu 702-701, Korea

Hyun-Wook Kwon[‡]

Graduate School, Mechanical Engineering Department, Kyungpook National University, Korea

Beom-Soo Lim^{‡†}

Agency for Defense Development, Korea

(Received March 23, 2004, Accepted September 15, 2004)

Abstract. A new load/displacement parameter method is proposed for the simultaneous control of applied loads and structural displacements at one or more points. The procedure is based on a generalized Riks' method, which utilizes load/displacement parameters as scaling factors to analyze post-buckling phenomena including snap-through or snap-back. The convergence characteristics are improved by employing new relaxation factors through an incremental displacement parameter, particularly in a region that exhibits severe numerical instability. The improved performance is illustrated by means of a numerical example.

Key words: post-buckling phenomena; snap-back phenomena; incremental load parameter; incremental displacement parameter; relaxation factor; relaxation method.

1. Introduction

The problems encountered with a large displacement in a finite element analysis are related to the nonlinear response. Many numerical methods without limit points have been proposed to solve these nonlinear problems. Among them, the Newton-Raphson method is recognized as quite effective. In this method, however, the solutions tend to be unstable and diverge near the limit point where the tangent stiffness becomes zero or infinite. Therefore, producing a numerical solution for a post-buckling problem using the Newton-Raphson method is difficult and almost impossible if the snap-back phenomenon occurs.

Several approaches (Wright and Gaylord 1968, Lock and Sabir 1973, Haisier *et al.* 1977, Mondkar and Powell 1978, Ramm 1981, Bergan 1979) have been developed to analyze such post-

[†] Professor, Corresponding author, E-mail: ydkwon@knu.ac.kr

[‡] Ph.D. Candidate

^{‡†} Senior Researcher

buckling problems: Riks' constant-arc-length method (normal plane constraint) (Riks 1979) and Crisfield's constant-arc-length method (spherical constraint) (Crisfield 1981) are among the most commonly known. Plus, many researchers (Padovan and Tovichakchaikul 1982, Endo *et al.* 1984, Riks 1984, Simo *et al.* 1986, Chrcielewski and Schmidt 1985, Batoz and Dhatt 1979, Koo *et al.* 1988, Park and Kang 2003, Wang 2003) have since improved on these methods.

Because Riks' method is based on load increments, it is difficult to apply when the displacements are controlled, or when the load and displacement are simultaneously controlled at many points. Furthermore, the solution may become unstable and substantial computing time is required for a near-the-limit point and points where the tangent stiffness is infinite.

This paper reviews Riks' constant-arc-length method for analyzing post-buckling problems and proposes a new load displacement parameter method for cases when loads are applied to one or more points and the displacements of the structure are simultaneously controlled at one or more points. To improve the computational efficiency and convergence characteristics in a region where severe numerical instability is exhibited, a "relaxation method" is also proposed based on modified incremental displacement parameters including two relaxation factors.

The proposed methods, the 'load-displacement parameter method' and 'relaxation method', were applied to several numerical examples including the snap-through and snap-back phenomena: a simple cantilever model clamped on one side, 2-dimensional right angle-frame model, Belleville spring model, and 3-dimensional curved shell. The convergence speed was compared for various displacement-load ratios as the relaxation factors were varied, and, as a result, the effective relaxation factor ranges were obtained.

2. Numerical method for post-buckling phenomena

The most frequently used iteration scheme for solving post-buckling phenomena is the Newton-type method that uses a load parameter. However, if the snap through or snap back phenomena are included in this method, the equilibrium equations usually break down near the limit point even if the load increment is small. To overcome this difficulty several procedures have been developed. Among them, Riks' constant-arc-length method (normal plane constraint) and Crisfield's constant-arc-length method (spherical constraint) are well known.

This section briefly reviews some variations of Riks' arc-length procedure for load control and then derives an equation for the case when the load and displacement are controlled simultaneously.

2.1 Riks' constant-arc-length method

In the load-controlled arc-length method, proposed by Riks and subsequently improved by Simo, the stiffness matrix is symmetric and the solution is obtained by satisfying the arc-length constraint. Fig. 1 represents the arc-length method proposed by Riks.

Let $\{t\}^{(1)}$ denote the tangent vector to the load-deflection curve at the beginning of the time step, which can be expressed in matrix form as

$$\{t\}^{(1)} = [\{\Delta U\}^{(1)T}; \Delta\lambda^{(1)}]^T \quad (1)$$

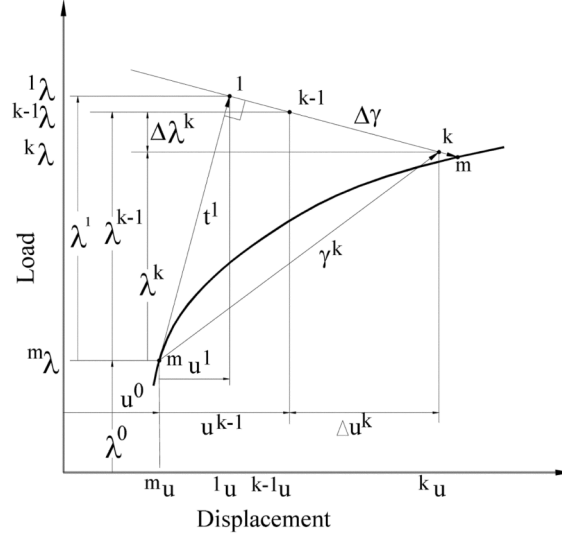


Fig. 1 Basic notation of Riks' method

where $\{\Delta U\}^{(1)} = \Delta\lambda^{(1)}\{\Delta U\}^{(0)}$ and $\Delta\lambda^{(1)}$ designates the load increment. When $k \geq 2$, $\{\Delta\gamma\}^{(k)}$ will represent the incremental vector defined by the matrix form as

$$\{\Delta\gamma\}^{(k)} = [\{\Delta U\}^{(k)T}; \Delta\lambda^{(k)}]^T \quad (2)$$

Riks' method requires the following constraint equation

$$\{t\}^{(1)T}\{\gamma\}^{(k)} = S_0^2 \quad (3)$$

where $\{t\}^{(1)}$ is the tangent vector, S_0 represents the prescribed value and $\{\gamma\}^{(k)}$ is the total incremental vector expressed as

$$\{\gamma\}^{(k)} = \{t\}^{(1)} + \sum_{n=2}^k \{\Delta\gamma\}^{(n)} \quad (4)$$

For improved computational efficiency, it is advantageous to enforce Eq. (3) as a two-step procedure, as follows:

$k = 1$. In the first iteration within a given increment, the constant arc constraint is enforced, which can be expressed as

$$\{t\}^{(1)T}\{t\}^{(1)} = S_0^2 \quad (5)$$

The substitution of Eq. (1) into Eq. (5) yields

$$\Delta\lambda^{(1)}\Delta\lambda^{(1)}\{\Delta U\}^{(0)T}\{\Delta U\}^{(0)} + \Delta\lambda^{(1)}\Delta\lambda^{(1)} = S_0^2 \quad (6)$$

Then, the load increment $\Delta\lambda^{(1)}$ becomes

$$\Delta\lambda^{(1)} = \left\{ \frac{S_0^2}{\{\Delta U\}^{(0)T} \{\Delta U\}^{(0)} + 1} \right\}^{1/2} \quad (7)$$

$k \geq 2$. The constant arc length constraint condition in Eq. (5) is only applied in the first step ($k = 1$) of the solution process. For $k \geq 2$ the normal plane constraint is enforced, which can be defined as

$$\{t\}^{(1)T} \{\Delta\gamma\}^{(k)} = 0 \quad (8)$$

The substitution of Eqs. (1) and (2) into Eq. (8) yields

$$\{\Delta U\}^{(1)T} \{\Delta U\}^{(k)} + \Delta\lambda^{(1)} \Delta\lambda^{(k)} = 0 \quad (9)$$

The substitution of the constraint Eq. (9) directly into the original system of equations results in a non-symmetric stiffness matrix. To overcome this drawback, a system of equations with a matrix coefficient is solved twice as follows (Simo *et al.* 1986). The formulation of an iterative solution procedure can be written as

$$[K]^{(k-1)} \{\Delta U\}^{(k)} = \Delta\lambda^{(k)} \{P\} + ({}^m\lambda + \lambda^{(k-1)}) \{P\} - \{F\}^{(k-1)} \quad (10)$$

where

- m : number of incremental stages
- k : number of iterations at current stage ($m + 1$)
- $[K]^{(k-1)}$: tangent matrix at iteration ($k - 1$)
- ${}^m\lambda$: load factor until incremental stage m
- $\lambda^{(k-1)}$: load factor until iteration $k - 1$ at current stage $m + 1$
- $\Delta\lambda^{(k)}$: load increment until iteration k at current stage $m + 1$
- $\{\Delta U\}^{(k)}$: incremental displacement vector until iteration k at current stage $m + 1$
- $\{P\}$: external load vector
- $\{F\}$: equivalent nodal force vector

Eq. (10) can be divided into the following two Eqs. (11) and (12)

$$[K]^{(k-1)} \{\Delta U_I\}^{(k)} = \{P\} \quad (11)$$

$$[K]^{(k-1)} \{\Delta U_{II}\}^{(k)} = ({}^m\lambda + \lambda^{(k-1)}) \{P\} - \{F\}^{(k-1)} \quad (12)$$

The incremental displacement vector at iteration k can be expressed as

$$\{\Delta U\}^{(k)} = \Delta\lambda^{(k)} \{\Delta U_I\}^{(k)} + \{\Delta U_{II}\}^{(k)} \quad (13)$$

The substitution of Eq. (13) into Eq. (9) yields

$$\Delta\lambda^{(k)} = - \frac{\{\Delta U\}^{(1)T} \{\Delta U_{II}\}^{(k)}}{\{\Delta U\}^{(1)T} \{\Delta U_I\}^{(k)} + \Delta\lambda^{(1)}} \quad (14)$$

Thereafter, Eqs. (7) and (14) can be converted as follows by incorporating the displacement scale factor, u^* , and load scale factor, p^* .

$$\Delta\lambda^{(1)} = \left\{ \frac{S_{0s}^2}{\{\Delta U_s\}^{(0)T} \{\Delta U_s\}^{(0)} + M/p^{*2}} \right\}^{1/2} \quad (15)$$

$$\Delta\lambda^{(k)} = -\frac{\{\Delta U_s\}^{(1)T} \{\Delta U_{IIs}\}^{(k)}}{\{\Delta U_s\}^{(1)T} \{\Delta U_{Is}\}^{(k)} + \Delta\lambda^{(1)}/p^{*2}} \quad (16)$$

where

$$\{\Delta U_s\}^{(1)} = \{\Delta U\}^{(1)}/u^*$$

$$\{\Delta U_{Is}\}^{(k)} = \{\Delta U_I\}^{(k)}/u^*$$

$$\{\Delta U_{IIs}\}^{(k)} = \{\Delta U_{II}\}^{(k)}/u^*$$

$$M = 1 \quad \text{or} \quad \text{D.O.F}/3$$

A stable solution can be obtained when $M = \text{D.O.F}/3$.

2.2 Problems with simultaneous load application and displacement control : Load-displacement parameter method

When either displacements are controlled at one or more points, or displacements and loads are simultaneously controlled, the previous load parameter method is insufficient to yield a solution. To overcome this, the current study presents a new parameter method.

In general, displacements are controlled at points p and q , and loads are applied at points i and j , as denoted by

$$\begin{aligned} \{U\} &= \{\bar{U}\}, \quad (U_p = \bar{U}_p, U_q = \bar{U}_q) \\ \{P\} &= \{\bar{P}\}, \quad (P_i = \bar{P}_i, P_j = \bar{P}_j) \end{aligned} \quad (17)$$

where $\{\bar{U}\}$ and $\{\bar{P}\}$ represent the relations between the constrained displacements and the loads. The displacements are unknown except for points p and q , and the loads are zero or unknown except for points i and j . The tangential vector $\{t\}^{(1)}$ at an arbitrary point on the load-displacement curve can be denoted with an incremental displacement vector and incremental load vector as

$$\{t\}^{(1)} = [\{\Delta U\}^{(1)T}; \{\Delta P_D\}^{(1)T}; \{\Delta P_L\}^{(1)T}]^T \quad (18)$$

where the subscript D represents the point where the displacement is controlled and subscript L corresponds to the point where the load is controlled. The displacement and load can both be converted into a scaled quantity using scale factors such as

$$\{U_s\} = \{U\}/u^* \quad (19)$$

$$\{P_s\} = \{P\}/p^* \quad (20)$$

Therefore, the scaled tangential vector $\{t_s\}^{(1)}$ at a point on the scaled load-displacement curve becomes

$$\{t_s\}^{(1)} = [\{\Delta U_s\}^{(1)T}; \{\Delta P_{D_s}\}^{(1)T}; \{\Delta P_{L_s}\}^{(1)T}]^T \quad (21)$$

where

$$\{\Delta U_s\}^{(1)} = \Delta\mu^{(1)}\{U_s\}^{(0)} \quad (22)$$

and $\Delta\mu$ is the displacement increment.

In addition, the scaled incremental vector, $\{\Delta\gamma_s\}^{(k)}$ can be defined by the matrix notation as

$$\{\Delta\gamma_s\}^{(k)} = [\{\Delta U_s\}^{(k)T}; \{\Delta P_{D_s}\}^{(k)T}; \{\Delta P_{L_s}\}^{(k)T}]^T \quad (23)$$

It is also possible to obtain Riks' constraint by using Eqs. (21) and (23) as Eq. (3) and it can be computed as a two-step, as in the previous procedure.

$k=1$. In the first iteration of the initial increment, the constant-arc-length constraint is

$$\{t_s\}^{(1)T}\{t_s\}^{(1)} = S_{0s}^2 \quad (24a)$$

This is accomplished by setting

$$\{\Delta U_s\}^{(1)T}\{\Delta U_s\}^{(1)} + \{\Delta P_{D_s}\}^{(1)T}\{\Delta P_{D_s}\}^{(1)} + \{\Delta P_{L_s}\}^{(1)T}\{\Delta P_{L_s}\}^{(1)} = S_{0s}^2 \quad (24b)$$

The scaled incremental displacement vector $\{\Delta U_s\}^{(1)}$ can be written as a product of the displacement increment $\Delta\mu^{(1)}$ and $\{U_s\}^{(0)}$:

Here $\{U_s\}^{(0)} = \{U_s\}^{(0)}/u^*$, and $\{U\}^{(0)}$ mean the displacement ratio vector that represents the ratio between the displacements in the structure, and can be obtained from

$$([\overset{t}{\underset{0}{K}}]^{(0)} + \alpha[D_t])\{U\}^{(0)} = \alpha\{\bar{U}\} + \kappa^*\{\bar{P}\} \quad (25)$$

where

$$\alpha \gg K_{ii}$$

$[D_t]$: unit diagonal matrix

$$\{\bar{U}\} = \{\dots \bar{U}_p \dots \bar{U}_q \dots\}^T, \quad \bar{U}_p = 1$$

The subscripts p and q denote the D.O.F. of the point where the displacements are controlled, therefore, the displacements at points other than these points are unknown. $\kappa^* = \Delta\lambda/\Delta\mu$ denotes the ratio that should be satisfied between the load increment and the displacement increment.

The scaled equivalent nodal force $\{\Delta P_{Ds}\}^{(1)}$ corresponding to $\{\Delta U_D\}^{(1)}$ becomes

$$\begin{aligned}\{\Delta P_{Ds}\}^{(1)} &= \{\Delta P_D\}^{(1)}/p^* \\ &= [{}^{t+\Delta t}{}_0\mathbf{K}]^{(0)}\{\Delta U_D\}^{(1)}/p^* \\ &= \Delta\mu^{(1)}[{}^{t+\Delta t}{}_0\mathbf{K}]^{(0)}\{U\}^{(0)}/p^*\end{aligned}\quad (26)$$

In contrast, the scaled incremental load vector $\{\Delta P_{Ls}\}$ can be expressed using the load increment $\Delta\lambda$ and the load scaling factor p^* as follows:

$$\begin{aligned}\{\Delta P_{Ls}\}^{(1)} &= \Delta\lambda^{(1)}\{\Delta P_{Ls}\}^{(0)} \\ &= \Delta\mu^{(1)}\kappa^*\{P_L\}^{(0)}/p^*\end{aligned}\quad (27)$$

The substitution of Eqs. (26), (27), into Eq. (24b) yields

$$\Delta\mu^{(1)} = \left[\frac{S_{0s}^2}{\{\{U_s\}^{(0)T}\{U_s\}^{(0)} + \{P_{Ds}\}^{(0)T}\{P_{Ds}\}^{(0)} + (\kappa^*/p^*)^2\}} \right]^{1/2}\quad (28)$$

where $\Delta\mu^{(1)}$ denotes the displacement increment at $k = 1$, and

$$\begin{aligned}\{P_{Ds}\}^{(0)} &= [{}^{t+\Delta t}{}_0\mathbf{K}]^{(0)}\{U\}^{(0)}/p^* \\ |\{P_L\}^{(0)}| &= 1\end{aligned}$$

$k \geq 2$. In a subsequent iteration, the normal plane constraint can be defined as

$$\{t_s\}^{(1)T}\{\Delta\gamma_s\}^{(k)} = 0\quad (29a)$$

Similarly, using Eqs. (21) and (23) the following expression can be given

$$\{\Delta U_s\}^{(1)T}\{\Delta U_s\}^{(k)} + \{\Delta P_{Ds}\}^{(1)T}\{\Delta P_{Ds}\}^{(k)} + \{\Delta P_{Ls}\}^{(1)T}\{\Delta P_{Ls}\}^{(k)} = 0\quad (29b)$$

A finite element equilibrium equation with a displacement constraint can also be rewritten as

$$\begin{aligned}\{[{}^{t+\Delta t}{}_0\mathbf{K}]^{(k-1)} + \alpha[D_t]\}\{\Delta U\}^{(k)} = \\ \Delta\mu^{(k)}(\alpha\{\bar{U}\} + \kappa^*\{\bar{P}\}) + ({}^m\mu + \mu^{(k-1)})\kappa^*\{\bar{P}\} - \{{}^{t+\Delta t}{}_0F\}^{(k-1)}\end{aligned}\quad (30)$$

To overcome the drawback resulting in the non-symmetric coefficient matrix in Eq. (30), the system of equations can be solved in two steps as in Eqs. (11) and (12).

$$\begin{aligned} \{[{}^{t+\Delta t}{}_0\mathbf{K}]^{(k-1)} + \alpha[\mathbf{D}_I]\}\{\Delta U_I\}^{(k)} &= \alpha\{\bar{U}\} + \kappa^*\{\bar{P}\} \\ \{[{}^{t+\Delta t}{}_0\mathbf{K}]^{(k-1)} + \alpha[\mathbf{D}_I]\}\{\Delta U_{IE}\}^{(k)} &= ({}^m\mu + \mu^{(k-1)})\kappa^*\{\bar{P}\} - \{{}^{t+\Delta t}{}_0\mathbf{F}\}^{(k-1)} \end{aligned} \quad (31)$$

and $\{\Delta U_I\}^{(k)}$, $\{\Delta U_{IE}\}^{(k)}$ are obtained from Eq. (31).

The incremental displacement vector $\{\Delta U_s\}^{(k)}$ can be written as

$$\{\Delta U_s\}^{(k)} = \{\Delta U_{Ds}\}^{(k)} + \{\Delta U_{Es}\}^{(k)} \quad (32)$$

$$\{\Delta U_{Ds}\}^{(k)} = \Delta\mu^{(k)}\{\Delta U_{IDs}\}^{(k)}$$

$$\{\Delta U_{Es}\}^{(k)} = \Delta\mu^{(k)}\{\Delta U_{IEs}\}^{(k)} + \{\Delta U_{IEs}\}^{(k)} \quad (33)$$

The substitution of Eq. (33) into Eq. (32) yields

$$\{\Delta U_s\}^{(k)} = \Delta\mu^{(k)}\{\Delta U_{Is}\}^{(k)} + \{\Delta U_{IEs}\}^{(k)} \quad (34)$$

where $\{\Delta U_{Is}\}^{(k)} = \{\Delta U_I\}^{(k)}/u^*$, $\{\Delta U_{IEs}\}^{(k)} = \{\Delta U_{IE}\}^{(k)}/u^*$ and E means the point where the displacements are not controlled.

The incremental load vectors of the points where the displacement and load are controlled, $\{\Delta P_{Ds}\}^{(k)}$ and $\{\Delta P_{Ls}\}^{(k)}$, can be denoted by using the displacement increment $\Delta\mu^{(k)}$ as follows:

$$\begin{aligned} \{\Delta P_{Ds}\}^{(k)} &= \{\Delta P_D\}^{(k)}/p^* \\ &= [{}^{t+\Delta t}{}_0\mathbf{K}]^{(k-1)}\{\Delta U_D\}^{(k)}/p^* \\ &= \Delta\mu^{(k)}[{}^{t+\Delta t}{}_0\mathbf{K}]^{(k-1)}\{\Delta U_{ID}\}^{(k)}/p^* \end{aligned} \quad (35)$$

$$\{\Delta P_{Ls}\}^{(k)} = \Delta\mu^{(k)}\kappa^*\{P_L\}/p^* \quad (36)$$

Finally using Eqs. (29)-(36), the displacement increment $\Delta\mu^{(k)}$ can be obtained from

$$\begin{aligned} \Delta\mu^{(k)} &= -\{\Delta U_s\}^{(1)T}\{\Delta U_{IEs}\}^{(k)}/[\{\Delta U_s\}^{(1)T}\{\Delta U_{Is}\}^{(k)} + \\ &\quad \{\Delta P_{Ds}\}^{(1)T}\{\Delta P_{IDs}\}^{(k)} + \Delta\mu^{(1)}(\kappa^*/p^*)^2] \end{aligned} \quad (37)$$

where

$$\{\Delta U_s\}^{(1)} = \Delta\mu^{(1)}\{U\}^{(0)}/u^*$$

$$\{\Delta P_{Ds}\}^{(1)} = \Delta\mu^{(1)}\{P_D\}^{(0)}/p^* = \Delta\mu^{(1)}[\mathbf{K}]^{(0)}\{U\}^{(0)}/p^*$$

$$\{\Delta P_{IDs}\}^{(k)} = [\mathbf{K}]^{(k-1)}\{\Delta U_{ID}\}^{(k)}/p^*$$

According to this method, the load increment is expressed as a ratio of the displacement

increment. As a result, the loads and displacements can be simultaneously controlled by just the displacement increment.

Since Eq. (37) is a very general expression, many cases can be derived using this equation. The elimination of the terms related to displacement control, (p, q) , and the multiplication of $\kappa^*(=\Delta\lambda/\Delta\mu)$ at both hands in Eq. (37), produce Riks' method (Bergan 1979) for a load control problem as

$$\Delta\lambda^{(k)} = -\frac{\{\Delta U_s\}^{(1)T}\{\Delta U_{II_s}\}^{(k)}}{\{\Delta U_s\}^{(1)T}\{\Delta U_{Is}\}^{(k)} + \Delta\lambda^{(1)}/p^{*2}} \quad (37a)$$

The elimination of the terms related to load control, (i, j) , yields a Riks' type method (Endo *et al.* 1984) for a displacement control problem as

$$\Delta\mu^{(k)} = -\{\Delta U_s\}^{(1)T}\{\Delta U_{II_s}\}^{(k)}/[\{\Delta U_s\}^{(1)T}\{\Delta U_{Is}\}^{(k)} + \{\Delta P_{Ds}\}^{(1)T}\{\Delta P_{ID_s}\}^{(k)}] \quad (37b)$$

The solution for a load control problem can be obtained by taking $u^* \rightarrow \infty$ in Eq. (37a), and this equation becomes the Newton-Raphson method (Bathe 1982) as

$$\Delta\lambda^{(k)} = 0 \quad (37c)$$

The substitution of p^* for the infinity condition in Eq. (37a) yields the following, which is Ramm's method¹⁾ or Crisfield's quasi-penalty method (Crisfield 1981).

$$\Delta\lambda^{(k)} = -\{\Delta U_s\}^{(1)T}\{\Delta U_{II_s}\}^{(k)}/\{\Delta U_s\}^{(1)T}\{\Delta U_{Is}\}^{(k)} \quad (37d)$$

By considering only i -D.O.F. in Eq. (37d), one obtains Batoz's method (Batoz and Dhatt 1979) as

$$\Delta\lambda^{(k)} = -\{\Delta U_{II_i}\}^{(k)}/\{\Delta U_{I_i}\}^{(k)} \quad (37e)$$

The control of p^* in Eq. (37a) reduces it to Noor and Peters' method (Noor and Peters 1981).

The elimination of the load term and the substitution of u^* for ∞ in Eq. (37b) give the solution for a displacement control problem as

$$\Delta\mu^{(k)} = -\{\Delta U_s\}^{(1)T}\{\Delta U_{II_s}\}^{(k)}/\{\Delta U_s\}^{(1)T}\{\Delta U_{Is}\}^{(k)} \quad (37f)$$

and this has become the quasi-penalty method (Choi *et al.* 1990).

Considering only p -D.O.F. in Eq. (37f), produces the penalty method (Choi *et al.* 1990) as

$$\Delta\mu^{(k)} = 0 \quad (37g)$$

Therefore, Eq. (37) can be regarded as a general equation including most cases.

2.3 New approach : Relaxation method

The cases in which loads and displacements are controlled simultaneously in a post-buckling problem can be analyzed by the load_displacement parameter method, as stated previously in

section 2.2, however, the solution is unstable near the limit point or at the point where the tangent stiffness is infinite. Accordingly, the present study proposes a new control parameter, $\Delta\mu_r^{(k)}$, incorporating two relaxation factors, β_1 and β_2 .

The third iteration in a total sense, that is the second iteration in equilibrium (normal constraint iteration) is apt to be unstable, because the starting point after the second iteration can be far from the exact equilibrium point. Thus, it is necessary that the third iteration should be relaxed for convergence.

Based on the current authors' experience, when the third iteration is not relaxed and diverges, any other effort at the following iteration stage is of no use. Although, the subsequent iterations are not as critical as the third one, relaxation is still required for better convergence. By watching the initial difference between the external and equivalent nodal load at each iteration stage, the relaxation factor can be confirmed. The displacement increment modified by the multiplication of the two relaxation factors yields:

$$\Delta\mu_r^{(k)} = -\{\Delta U_s\}^{(1)T} \{\Delta U_{IIEs}\}^{(k)} / [\{\Delta U_s\}^{(1)T} \{\Delta U_{Is}\}^{(k)} + \{\Delta P_{Ds}\}^{(1)T} \{\Delta P_{IDs}\}^{(k)} + \Delta\mu^{(1)} (\kappa^*/p^*)^2] \times f_1 \times f_2 \quad (38)$$

where f_1 and f_2 are obtained by using the relaxation factors β_1 and β_2 as

$$f_1 = \begin{cases} \beta_1: k = 3 & \text{and } kflag = 1 \\ 1: k \neq 3 & \text{or } kflag = 0 \end{cases}$$

$$f_2 = \begin{cases} \beta_2^n: k \geq 3 & \text{and } kflag = 1 \\ 1: k \leq 2 & \text{or } kflag = 0 \end{cases}$$

where

$$kflag = \begin{cases} 0: R_k < 1.0 & \text{for all } k \text{ at previous stage} \\ 1: R_k \geq 1.0 & \text{for any } k \text{ at previous stage} \end{cases}$$

$$n = \begin{cases} 1: R_k > 1 \\ 2: R_k > 5 \\ 3: R_k > 10 \end{cases}$$

where R_k is the ratio of initial errors between the previous stage and the present stage, and the errors are the maximum difference between the applied load and the equivalent nodal force at all nodes.

The condition of convergence is $\Delta\mu_r^{(k)}/\Delta\mu_r^{(1)} < \varepsilon$ and the displacement and nodal force after convergence can be obtained as follows

$$\begin{aligned} \{{}^{t+\Delta t}U\} &= \{{}^tU\} + \{\Delta U\}^{(1)} + \{\Delta U\}^{(2)} + \dots \\ \{{}^{t+\Delta t}P\} &= \{{}^{t+\Delta t}_0F\}^{(k)} \end{aligned} \quad (39)$$

In the above, β_1 controls the quantity of the displacement increment in the next stage, if the convergence is unstable in the previous stage. That is, if the convergence is unstable in the $(m-1)^{\text{th}}$ stage, the first displacement increment in the m^{th} stage is controlled by multiplying with β_1 . In the case when the solution cannot converge by any means because the first incremental stage diverged, the modification factor β_1 is required for convergence. Through this control, we can prevent that the m^{th} incremental stage is affected in convergence by instability of the $(m-1)^{\text{th}}$ incremental stage, therefore convergence near limit points can be fairly improved.

However, since it is impossible to completely resolve the instability of the convergence in the m^{th} incremental stage with only the use of β_1 , the second relaxation factor β_2 is required in order to modify the displacement increment in the subsequent iteration stages. In the convergence process, the solution can be estimated using the ratio between the initial error in the previous iteration stage and that in the current iteration stage. If the ratio is bigger than unity, the increment of the next stage should be relaxed using β_2 and an effective displacement increment can then be selected.

The computation process explained in sections 2.2 and 2.3 can be summarized as follows:

- 1) Given the displacement component \bar{U}_p, \bar{U}_q to be controlled, and applied loads \bar{P}_i, \bar{P}_j .
- 2) Decide normal arc-length S_0 .
- 3) Compute initial stiffness matrix $[\ ^{t+\Delta t}_0 K]^{(0)}$ in tangential direction and equivalent nodal force vector $[\ ^{t+\Delta t}_0 F]^{(0)}$.
- 4) Solve the equation in two steps.
- 5) In the first step
 - a) Compute $\{U\}^{(0)}$.
 - b) Compute the load $\{P\}^{(0)}$ corresponding to $\{U\}^{(0)}$.
 - c) Compute $\{P_D\}^{(0)}$.
 - d) Compute the displacement increment $\Delta\mu^{(1)}$.
 - e) Obtain $\{^{t+\Delta t}U\}^{(1)}$ using the displacement increment.
 - f) Compute $[\ ^{t+\Delta t}_0 K]^{(0)}$ and $[\ ^{t+\Delta t}_0 F]^{(0)}$.
- 6) In the second step
 - a) Compute $\{\Delta U_I\}^{(k)}$ and $\{\Delta U_{II}\}^{(k)}$ from the equilibrium equation divided into two parts.
 - b) Obtain $\{P_D\}^{(k)}$.
 - c) Apply the relaxation factor as follows.
 - (1) Decide the first relaxation factor β_1 referring to the convergence in the previous iteration stage.
 - (2) Decide the second relaxation factor β_2 according to the ratio of errors between the previous iteration stage and the current iteration stage.
 - d) Compute the modified displacement increment $\Delta\mu_r^{(1)}$ using the relaxation factors.
- 7) Compute $\{^{t+\Delta t}U\}^{(k)}$ using the modified displacement increment.
- 8) Compute $[\ ^{t+\Delta t}_0 K]^{(k)}$ and $[\ ^{t+\Delta t}_0 F]^{(k)}$.
- 9) Check the convergence and loop stage 6)–9) until the convergence condition is satisfied.
- 10) if the convergence condition is satisfied, set

$$\{^{t+\Delta t}U\} = \{^{t+\Delta t}U\}^{(k)}$$

$$\{^{t+\Delta t}P\} = \{^{t+\Delta t}F\}^{(k)}$$

- 11) Increase the increment stage and go to stage 3).

3. Numerical examples and discussion

To establish the validity and applicability of the proposed analysis for problems in which loads and displacements are controlled simultaneously, a cantilever, right-angle frame, and hinged cylindrical shell were employed as numerical models. In addition, the Belleville spring model with a displacement control of multiple points was computed. To illustrate the relaxation method currently proposed, finite element analyses for the right angle frame and hinged cylindrical shell model were carried out for several ratios between the load and the displacement. Through the examples proper ranges for the relaxation factors are obtained and the effectiveness of the proposed method in increasing the computational convergence rate is demonstrated.

3.1 Load/displacement parameter method

3.1.1 Cantilever model

The material and geometric properties of the cantilever model are given in Fig. 2. The load was applied near the center, and the displacement was controlled at the end point. The finite element model was discretized into five 8-node isoparametric elements assuming plane stress and a linear elastic material.

The computed results of the cantilever model, shown in Fig. 2, were compared with those when the load was only applied at one point (A of Fig. 2). The one point load problem was then analyzed using Riks' method, whereas the case of the simultaneous control of the loads and the displacements was analyzed using the proposed load/displacement parameter method. In the above, the ratio between the load increment and the displacement increment was controlled at a constant ($\kappa^* = 50$).

In the case where the load and displacement were controlled simultaneously, as in Fig. 3, the curve moved to the position of increasing the displacement of point A for the same load because of controlling the displacement at point B. Fig. 4 shows that the ratio between the load applied to point A and the displacement applied to point B satisfied the given constant value. The force equilibrium condition was satisfied such that the relative difference between the external force and the equivalent nodal force was less than 10^{-4} . Accordingly, the validity of the proposed analysis method was confirmed for a load and displacement control problem.

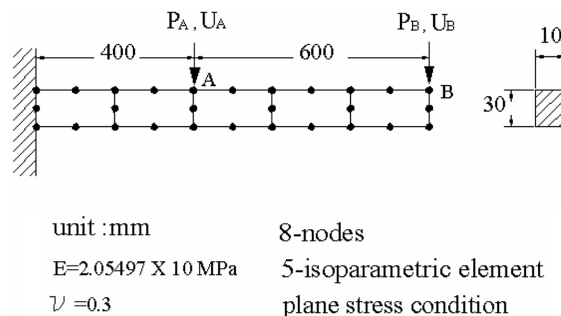


Fig. 2 Geometry and finite element model of cantilever

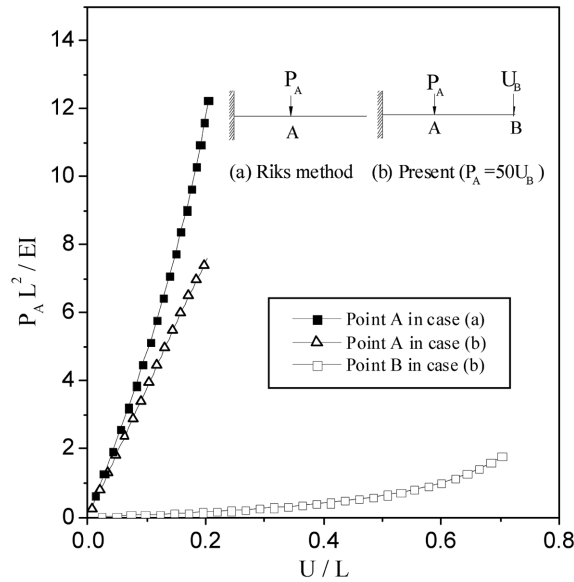


Fig. 3 Large displacement analysis of cantilever using proposed load/displacement parameter method

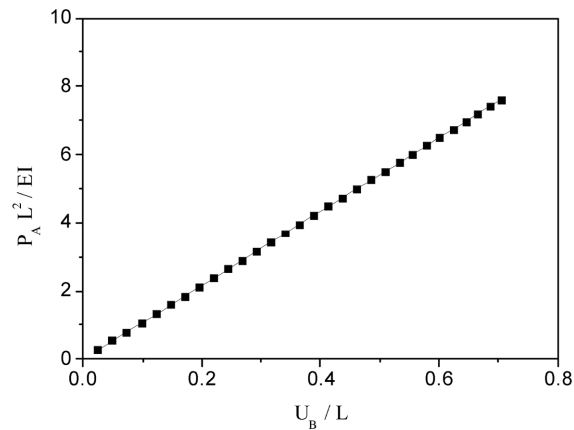


Fig. 4 Relation between load increments and displacement increment at each time step

3.1.2 Right-angle frame model

As the second example, a right-angle frame under plane stress conditions was considered so that the displacement was controlled at point A, and load applied at point B. The geometry and data for this problem are shown in Fig. 5. Eleven 8-node isoparametric 2-dimensional elements were used to discretize a finite element model of the right-angle frame, and the ratio of the load increment to the displacement increment was set as $\kappa^* = 3$.

Fig. 6 illustrates the displacement-load curve of point A, and shows that the solution converged very well even when the snap-back phenomenon occurred. Fig. 7 shows that the ratio of the load increment to the displacement increment remained at the initial constant value.

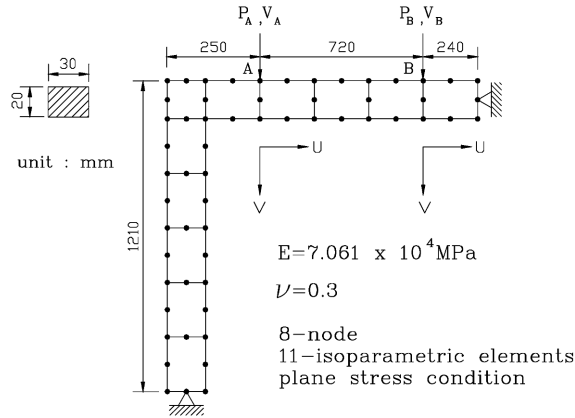


Fig. 5 Geometry and finite element model of right-angle frame

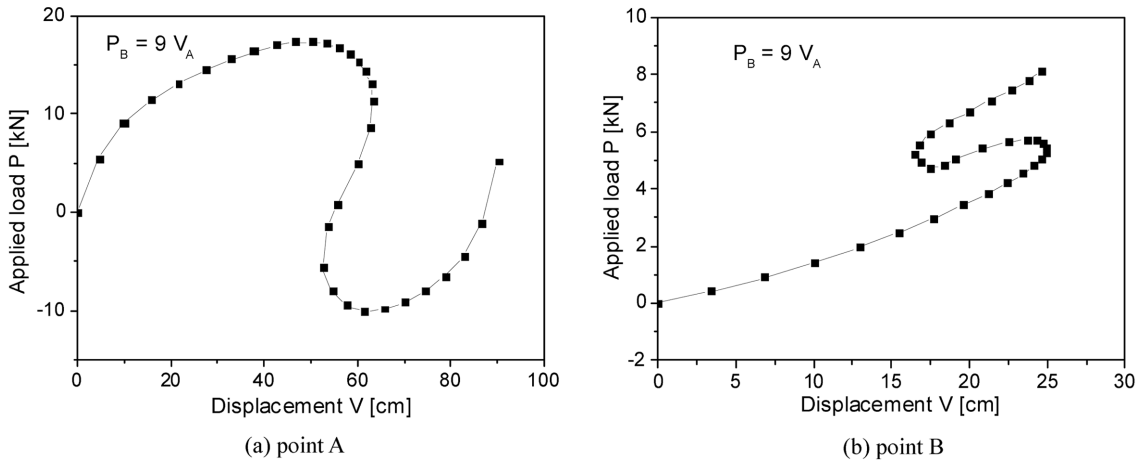


Fig. 6 Load-displacement curve of right-angle frame under load/displacement control

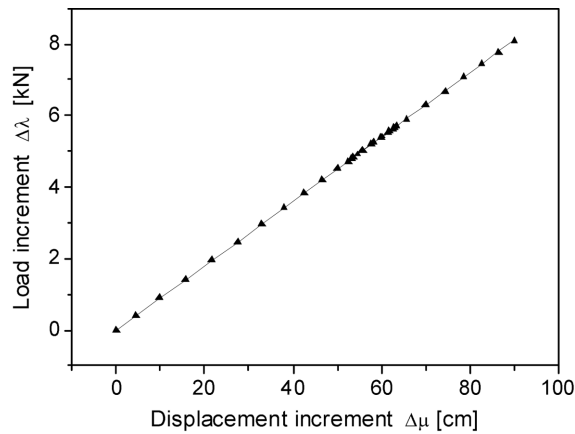


Fig. 7 Relation between load increments and displacement increments at each time step

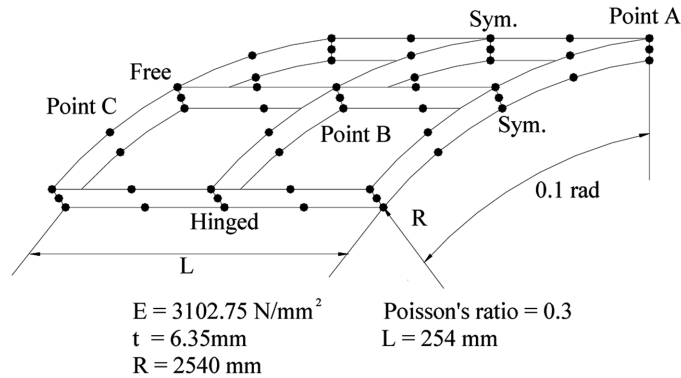


Fig. 8 Geometry and finite element model of hinged cylindrical shell

3.1.3 Hinged cylindrical shell model

The hinged elastic cylindrical shell, shown in Fig. 8, is a widely used problem for limit point algorithms and large displacement finite element formulations. Only a quarter of the shell needs to be modeled because of its symmetric properties, therefore, four 20-nodes isoparametric 3-D elements were used. The shell was free to rotate about its straight edges, however, these edges were otherwise completely restrained. The boundary conditions were free along the curved edges. The applied load and controlled displacement were vertical and the material was assumed to be linearly elastic.

In Fig. 9, the load-deflection relation resulting from the present work was compared with that obtained by ABAQUS, a commercial finite element program, for the case when the load was applied at point A. The structure exhibited a limit point corresponding with the load of approximately 540 N and exhibited snap-through as well as snap-back behavior. The two curves agreed very well with each other.

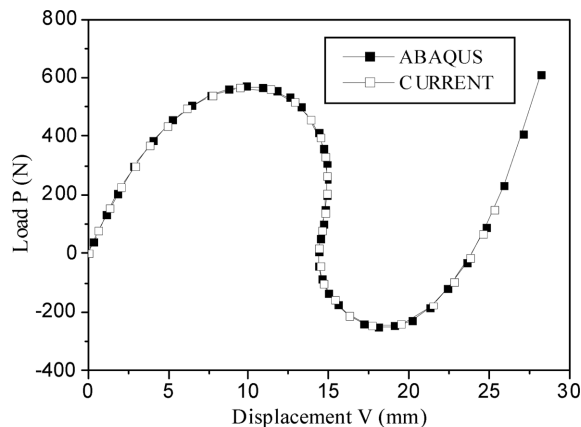


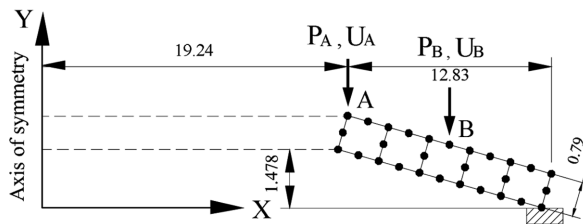
Fig. 9 Load-displacement curve of hinged cylindrical shell

3.1.4 Multi-point displacement controlled model

A Belleville spring, as seen in an automotive clutch, is a good example for displaying the snap-through phenomenon. In this example, a Belleville spring was analyzed under multi-point displacement control using the proposed method.

Fig. 10 shows the dimensions and finite element model of an axisymmetric Belleville spring. Five 8-node isoparametric elements were used to discretize a cross section of the structure.

Where displacements are controlled at many points, as in this case, problems are very difficult to analyze using the conventional Riks' method. However, this situation can be analyzed by the proposed displacement parameter method. To examine the validity of the multi-point displacement control method using Eq. (37), the displacement ratio between points A and B was set to 2:1. Fig. 11 shows the load-displacement curve. As a result, the displacement ratio between points A and B was maintained at 2:1. When the relative difference between the external force and the equivalent nodal force was smaller than 10^{-4} , the equilibrium condition was regarded as satisfied.



unit :mm 5 8-nodes
 E=2.05497 X 10 MPa 5-isoparametric element
 $\nu = 0.3$ axisymmetry condition

Fig. 10 Geometry and finite element model of Belleville spring

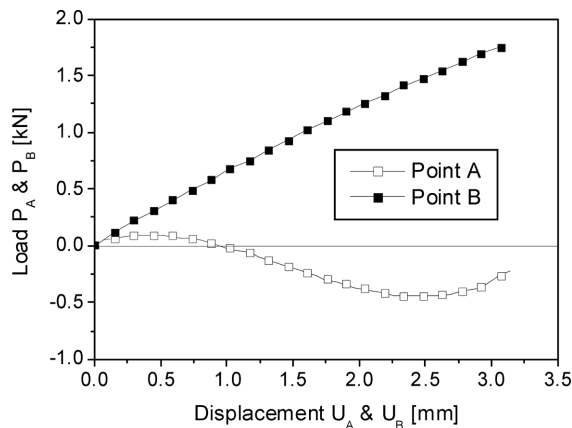


Fig. 11 Load-displacement curve of Belleville spring under displacement control

3.2 Relaxation method

The effectiveness of the relaxation factors was investigated using the right-angle frame model and 3-dimensional cylindrical shell model. First, the right-angle frame model was analyzed for the various conditions of the load/displacement ratio, κ^* ($\kappa^* = 0, 1, 3, 10, 30$), for which the displacement was controlled at point A and the load applied at point B, as shown in Fig. 5. The convergence was unstable because of the snap-back phenomenon occurring at point A, for all conditions of the load/displacement ratio. However, it became stable with the proper range of relaxation factors. Fig. 12 shows the iteration number for the various conditions.

Fig. 12(a) shows the improvement of the convergence with the proper range of relaxation factors in the case of $\kappa^* = 0$, that is, only the displacement was controlled. The convergence was improved by 24% when compared to the case where no relaxation factors were used. Fig. 12(b) represents $\kappa^* = 1$, where the load and displacement were controlled simultaneously with a small ratio. This case is more complex than when only the displacement is controlled, however, the solution converged very well with the proper range of relaxation factors. The convergence was improved by 34% when compared to the case where no relaxation factors were used.

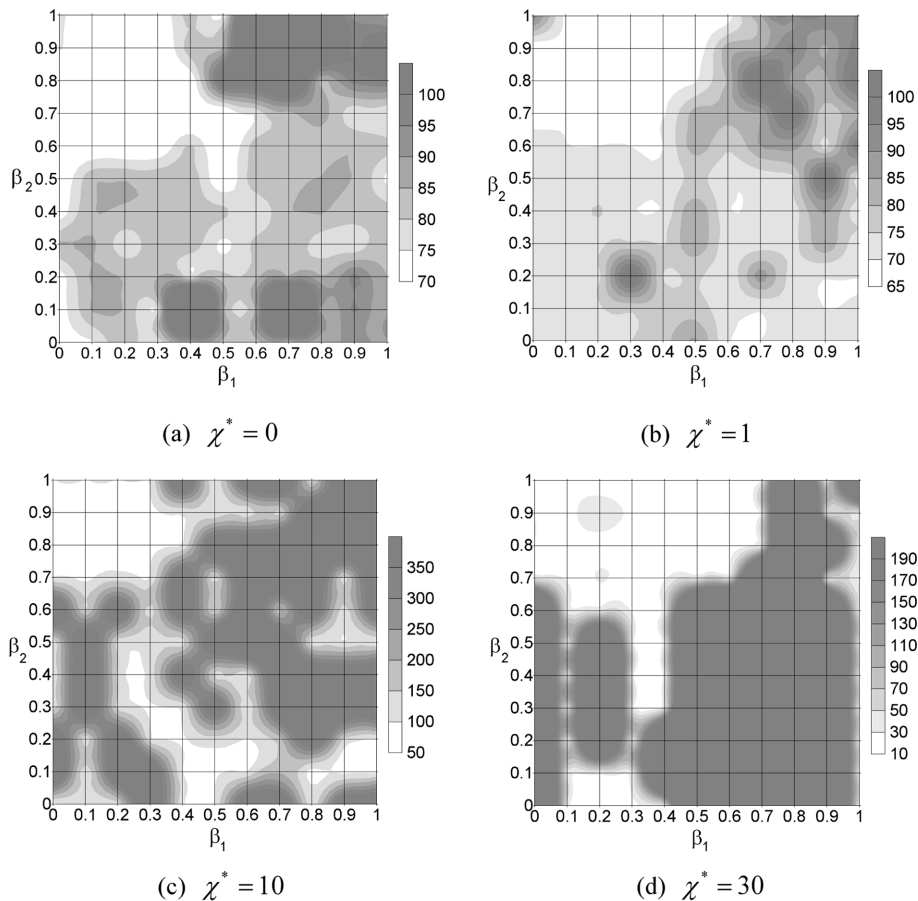


Fig. 12 Dither diagram of the iteration number of right-angle frame

Figs. 12(c) and (d) represent the cases of $\kappa^* = 10$ and $\kappa^* = 30$, respectively. Here, the loads were very large and there were several limit points on the load/displacement curve. In these cases, the solution using the load/displacement increment method by itself would either stop or diverge near the limit point. In contrast, the solution with the load/displacement increment method modified by the incorporation of relaxation factors exhibited a stable convergence.

Table 1 shows the iteration number taken for each analysis of the right-angle frame model. The

Table 1 Comparison of iteration numbers for each parameter

κ^*	(Unit: Number of iterations)		
	Not relaxed	Relaxed	Reduction ratio (%)
0	87	66	24
1	96	63	34
3	128	100	21
10	Failed	70	100
30	Failed	24	100

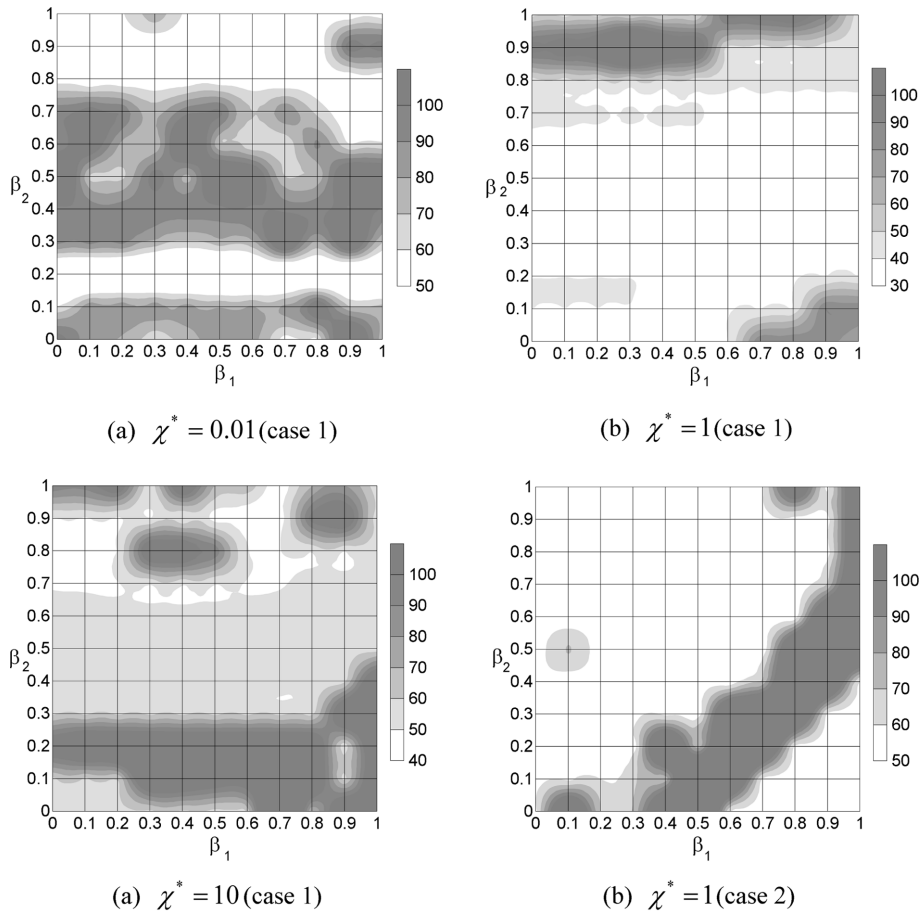


Fig. 13 Dither diagram of the iteration number of hinged cylindrical shell

improvement of the iteration numbers is shown by the percentage (%) when comparing the results of the modified load/displacement increment method, through relaxation, with those of the non-modified load/displacement increment method.

Figs. 13(a), (b), and (c) present the iteration numbers for the full range of relaxation factors of $\kappa^* = 0.01, 1, \text{ and } 10$, respectively, where the displacement is controlled at point A and the load applied at point B for the hinged cylindrical shell shown in Fig. 8. Fig. 13(d) displays the case when the displacement is controlled at point A and the load applied at point C in the same model $\kappa^* = 1$. In Fig. 13, the white area indicates the region of rapid convergence, and in most cases an improved convergence was accomplished by the use of a proper range of relaxation factors.

4. Conclusions

A load-displacement parameter method was developed for the post-buckling analysis of problems when loads are applied and displacements of structure are controlled simultaneously, plus a relaxation method was proposed to improve the stability and convergence of the solution. Based on several numerical examples, the following was concluded:

- 1) A new post-buckling analysis method designed for problems where loads/displacements are controlled simultaneously was derived based on the conventional Riks' method.
- 2) The proposed method is a general solution method including most previously developed post-buckling analysis methods (load control or displacement control).
- 3) When analyses of problem with snap-back phenomenon were carried out using the proposed load/displacement parameter method by itself, a solution was apt to exhibit instability around the limit point or the point where the load suddenly changes in comparison with the displacement. Accordingly, a new method based on incorporating two relaxation factors into load/displacement increments was developed which then improved the effectiveness and convergence of the solutions. The efficiency of this method was illustrated through numerical examples.
- 4) The proper ranges of the relaxation factors were determined as a result of computation for various conditions. The effective range was 0.0 to 0.3 for β_1 and 0.6 to 1.0 for β_2 .
- 5) When the modified load/displacement increment method with relaxation parameters was applied to an example, the iteration numbers were decreased by at least 21 %, when compared with those of the load/displacement method by itself.

Acknowledgements

This work was supported by the Brain Korea 21 Project in 2004.

References

- Bathe, K.J. (1982), *Finite Element Procedure in Engineering Analysis*, Prentice-Hall.
Batoz, J.L. and Dhatt, G. (1979), "Incremental displacement algorithms for nonlinear problems", *Int. J. Num. Meth. Engng.*, **14**, 1262-1267.

- Bergan, P.G. (1979), "Solution algorithms for nonlinear structural problems", *Proc. of the Int. Conf. on Engineering Applications of the Finite element Method*, Høfvik, Norway, A.S., Computas, 1-38.
- Choi, J.M., Jeong, Y.T., Yun, T.H. and Kwon, Y.D. (1990), "Finite element analysis of post-buckling phenomena using adaptive load/displacement parameter", *KSME*, **14**(3), 503-512.
- Chrcielewski, J. and Schmidt, R.A. (1985), "Solution control method for nonlinear finite element post-buckling analysis of structures", *Proc. of the EUROMECH Colloquium 200*, 19-33.
- Crisfield, M.A. (1981), "A fast incremental/iterative solution procedure that handles snap-through", *Comput. Struct.*, **13**, 55-62.
- Endo, T., Oden, J.T., Becker, E.B. and Miller, T. (1984), "A numerical analysis of contact and limit point behavior in a class of problems of finite elastic deformation", *Comput. Struct.*, **18**, 899-910.
- Haisier, W., Stricklin, J. and Key, J. (1977), "Displacement incrementation in nonlinear structural analysis by the self-correcting methods", *Int. J. Num. Meth. Engng.*, **11**, 3-10.
- Koo, J.S., Lee, B.C. and Kwak, B.M. (1988), "A study on improving efficiency in computational procedure of finite element nonlinear analysis of plane frame structures", *KSME*, **12**(4), 631-641.
- Lock, A.C. and Sabir, A.B. (1973), *Algorithm for Large Deflection Geometrically Nonlinear Plate and Curved Structures, in Mathematics of Finite Elements and Applications*, New York: Academic Press, 483-494.
- Mondkar, D.P. and Powell, G.H. (1978), "Evaluation of solution schemes for non-linear structures", *Comput. Struct.*, 223-236.
- Noor, A.K. and Peters, J.M. (1981), "Tracing post-limit-point with reduced basis technique", *Comput. Meth. Appl. Mech. Eng.*, **28**, 217-240.
- Padovan, J. and Tovichakchaikul, S. (1982), "Self-adaptive predictor-corrector algorithms for static non-linear structural analysis", *Comput. Struct.*, **15**, 365-377.
- Park, J.S. and Kang, Y.J. (2003), "Lateral buckling of beams with top bracing", *Struct. Eng. Mech.*, **16**(5), 613-625.
- Ramm, E. (1981), "Strategies for tracing the nonlinear response near limit points", *Proc. of the Europe-U.S. Workshop on Nonlinear Finite Element Analysis in Structural Mechanics*, Bochum, Germany: Springer-Verlag.
- Riks, E. (1979), "An incremental approach to the solution of snapping and buckling problems", *Int. J. Solids Struct.*, **15**, 529-551.
- Riks, E. (1984), "Some computational aspects of the stability analysis of nonlinear structures", *Comput. Meth. Appl. Mech. Eng.*, **47**, 219-259.
- Simo, J.C., Wriggers, P., Schweizwerhof, K.H. and Taylor, R.L. (1986), "Finite deformation post-buckling analysis involving inelasticity and contact constraints", *Int. J. Num. Meth. Engng.*, **23**, 779-800.
- Wang, Q. (2003), "On complex flutter and buckling analysis of a beam structure subjected to static follower force", *Struct. Eng. Mech.*, **16**(5), 533-556.
- Wright, E.W. and Gaylord, E.H. (1968), "Analysis of unbraced multistory steel rigid frames", *Proc. of the ASCE, J. Struct. Div.*, **94**, 1143-1163.